Cast iron coins of Song dynasty China: a metallurgical study

Michael L Wayman and Helen Wang

ABSTRACT: A selection of 37 Song dynasty Chinese cast iron coins was subjected to metallurgical analysis. From inscriptions, these are dated between 1078 and 1215 AD, and the mint locations of 23 of the coins are known. All were found to be white cast irons, but they separated into two types, one with relatively high levels of silicon, phosphorus and sulphur and divorced eutectic microstructures, and the other with low levels of these three elements and ledeburitic microstructures. Those coins that were minted in Shaanxi were all found to be of the first type, while those minted in the Hubei/Anhui region to the southeast are all of the second type. On the basis of sulphur content it is believed to be likely that iron used for the first group was smelted in coal- or coke-fired blast furnaces, while the iron in the second group was smelted using charcoal. This is in general agreement with what is known of the iron industry in China during the Song period.

Introduction

Analysis of objects from the past is often useful in providing information about aspects of life in earlier times and in this regard studies of coins have particular advantages. The date and location data they can convey, combined with the results of metallurgical analysis, have the potential to offer information that is important and relevant far beyond the field of numismatics. In the present work the main concern is with metallurgical and processing issues.

Here a selection of 37 Song dynasty cast iron coins from the collections of the Department of Coins and Medals, British Museum has been subjected to metallurgical analysis. The coins range in date from the eleventh to the thirteenth centuries AD, but it is possible from the coin inscriptions to establish to within a few years the dates of the individual coins and in some cases to determine the locations of the mints where they were produced. Although based on a limited number of coins, the study allows an initial investigation of the production processes of cast iron and of iron coins, including chronological and geographical differences. These touch on specific questions, relating to:

- the characteristics of the cast iron used for coinage
- the iron production processes used
- the technology of coin production operations, including any heat treatment and/or mechanical processing carried out after casting
- chronological, geographical and mint variations among the coins
- comparison of Song dynasty coin-casting technology with contemporary Chinese non-coin cast ironwork.

Of course, metallurgical analysis of a much larger number of coins would be necessary to address these questions comprehensively; furthermore the methodology could potentially be extended to include issues such as comparisons with cast iron coins and non-coin ironwork from other regions of East and Southeast Asia.

This paper presents the Song dynasty coins in historical context, and the results of their analyses along with a discussion of those results and their possible significance.

Song dynasty iron coins

Although the vast majority of Chinese coins through the ages were cast in bronze or brass, small quantities of iron coins are known to have been made at least as early as AD 24, (Zhou Weirong 1999, D B Wagner, unpublished manuscript) and then during the Tang dynasty (AD 618–907) and the Five Dynasties period (AD 907–960). However, iron coin production became much more commonplace during the Song dynasty (AD 960–1279), when rapid commercial growth created a demand for large amounts of money (Yang 1952, Hartwell 1967a, von Glahn 1996). Shortages of raw materials, such as the copper and tin needed to make

Table 1: Coin data and dimensions.

Coin	BM Reg no	Reign period & issue	Mint mark	Reign period (AD)	Coin date (AD)	Mass (g)	Rim thickness (mm)	Coin diameter (mm)	Hole size (mm)
Northern Song									
cm7	1985.10-32.11	Yuanfeng Tongbao	-	1078-1085	-	11.54	2.5	33.6	6.8
cm8	1983.10-15.12	Yuanfeng Tongbao	-	1086-1093	-	12.95	2.8	34.4	7.2
cm9	1985.10-32.12	Yuanfeng Tongbao	-	1086-1093	-	13.04	2.9	32.5	7.2
cm10	1983.6-19.82	Zhenghe Tongbao	-	1111-1117	-	4.50	1.9	25.6	6.2
cm11	1985.10-32.28	Zhenghe Tongbao	-	1111-1117	-	8.87	2.5	31.4	6.7
cm12	1979.3-4.7	Xuanhe Tongbao	shaan	1119-1125	-	2.89	1.3	24.5	6.5
cm13	1883.7-1.899	Xuanhe Tongbao	shaan	1119-1125	-	3.49	1.2	25.1	6.5
cm17	1882.6-1.251	Xuanhe Tongbao	shaan	1119-1125	-	3.99	1.7	25.3	6.2
cm14	1985.10-32.33	Xuanhe Tongbao	shaan	1119-1125	-	4.25	1.7	25.3	6.1
cm15	1983.6-19.83	Xuanhe Tongbao	shaan	1119-1125	-	4.01	1.6	25.0	6.2
cm16	1985.10-32.32	Xuanhe Tongbao	shaan	1119-1125	-	3.99	1.9	25.3	5.9
Southern Song									
cm18	1972.8-8.39	Qiandao Yuanbao	-	1165-1173	-	6.69	2.1	28.2	7.6
cm2	1983.6-19.84	Chunxi Yuanbao	dot in crescent	1174-1189	1174-1179	5.92	1.9	31.6	8.7
cm3	1972.8-8.42	Chunxi Yuanbao	-	1174-1189	1174-1179	5.61	1.9	31.6	8.5
cm19	1972.8-8.40	Chunxi Yuanbao	dot in crescent	1174-1189	1174-1179	8.04	2.1	31.8	8.4
cm20	1983.6-19.85	Chunxi Yuanbao	-	1174-1189	1174-1179	4.31	2.0	26.8	6.8
cm21	1972.8-8.41	Chunxi Yuanbao	-	1174-1189	1174-1179	7.55	2.0	31.5	8.2
cm30	1987.1-9.69	Chunxi Yuanbao	chun	1174-1189	1174-1179	6.73	2.1	27.7	6.6
cm33	1987.11-11.25	Chunxi Yuanbao	tong	1174-1189	1174-1179	6.57	2.0	29.4	6.3
cm32	1987.1-9.80	Chunxi Yuanbao	tong 12	1174-1189	1185	7.36	2.1	27.7	6.0
cm31	1987.1-9.75	Chunxi Yuanbao	chun 15	1174-1189	1188	6.87	2.1	27.7	7.0
cm34	1987.1-9.87	Shaoxi Tongbao	chun 1	1190-1194	1190	7.28	2.2	27.1	6.5
cm35	1987.1-9.88	Shaoxi Tongbao	chun 2	1190-1194	1191	6.70	2.1	28.5	5.6
cm36	1987.1-9.90	Shaoxi Tongbao	tong 2	1190-1194	1191	6.59	2.0	27.2	5.9
cm37	1996.2-17.697	Shaoxi Tongbao	tong 5	1190-1194	1194	6.70	2.1	29.1	6.1
cm6	1972.8-8.48	Qingyuan Tongbao	-	1195-1200	-	8.40	2.3	30.5	7.7
cm1	1979.2-30.2	Qingyuan Tongbao	-	1195-1200	-	5.24	1.9	29.0	6.5
cm28	1987.1-9.111	Jiading Tongbao	han 1	1208-1224	1208	7.21	2.2	27.8	5.3
cm29	1987.1-9.112	Jiading Tongbao	han 2	1208-1224	1209	8.08	2.3	27.9	4.9
cm22	1987.11-11.41	Jiading Tongbao	chun 2	1208-1224	1209	6.95	2.1	28.3	5.9
cm26	1987.1-9.109	Jiading Tongbao	tong 2	1208-1224	1209	7.02	2.2	28.4	6.1
cm5	1972.8-8.47	Jiading Xinbao	3	1208-1224	1210	11.25	2.9	34.3	9.5
cm27	1987.1-9.110	Jiading Tongbao	tong 3	1208-1224	1210	7.45	2.3	27.9	6.1
cm4	1972.8-8.45	Jiading Yuanbao	chun 3	1208-1224	1210	6.99	2.4	30.0	7.9
cm23	1987.11-11.42	Jiading Tongbao	chun 3	1208-1224	1210	6.04	2.0	27.8	6.0
cm24	1987.11-11.43	Jiading Tongbao	chun 4	1208-1224	1211	7.13	2.2	28.8	6.1
cm25	1987.11-11.44	Jiading Tongbao	chun 8	1208-1224	1215	7.08	2.5	27.0	6.7

bronze, are believed to be one of the major factors that stimulated the production of cast iron coinage. The advantages of using iron are obvious: iron ore was widely available, and cast iron is cheaper to produce than bronze. On the other hand poor resistance to corrosion in many environments and the relative difficulty of obtaining a fine impression has kept cast iron from becoming a viable competitor to copper-based coinage materials under most sets of circumstances. There was a well-developed iron industry in China, as well as a long history of fine casting, and the technology for casting bronze coins could be applied to the casting of iron coins.

Iron coin production in Song dynasty China was neither homogeneous nor static. In general, it appears that during the Northern Song period (AD 960–1127) mints in different localities produced either bronze coins or iron coins, and in some cases both (Peng Xinwei 1965). During the Southern Song period (AD 1127–1279) iron coins were circulated predominantly in Sichuan Province.

The volume of coin production also varied over time. The most intense period of production was the Yuanfeng reign period (1078–1085), during which the annual output has been estimated at over five million strings of bronze coins and one million strings of iron coins, with each string nominally holding 1000 coins. There were during this period 17 inspectorates (mints) for bronze coins and nine for iron coins; of the latter six were located in Shaanxi and three in Sichuan (Peng Xinwei 1965). Coin production dropped dramatically during the Southern Song period, in part because of the use of paper money.

Of the 37 Song dynasty iron coins selected for this study, 11 date from the Northern Song period and 26 from the Southern Song. The physical dimensions of the coins are given in Table 1. On the obverse of each coin is a four-character inscription. The first two characters indicate the reign period during which it was issued, localizing the date to within a 5 to 15-year period (Peng Xinwei 1965). The second two characters read 'tongbao', 'yuanbao' or 'xinbao', literally 'circulating treasure' or 'first treasure' or 'new treasure', respectively (Fig 1). On the reverse of some coins there is a one or two character inscription indicating the year of the reign period in which it was issued, and/or the mint where it was produced. For example the numeral 5 on a coin of the Shaoxi reign period (AD 1190–1194) refers to year 5 of that period (AD 1194). In the case of the Chunxi reign period (AD 1174–1189), year numbers were given to coins beginning in year 7 (AD 1180), so coins without numbers are taken as being within the range AD 1174–1179.

Experimental procedure

Examinations were carried out using optical and scanning electron metallography to characterize the microstructures of the coins. Compositional information was obtained by energy-dispersive X-ray microanalysis (EDX) in the scanning electron microscope (SEM). The coins were also subjected to X-radiography. Air path energy-dispersive X-ray fluorescence analysis (XRF) was used as required.

The cutting of metallographic cross-sections in order to characterize the material was not permitted in the case of these coins, which have display and study value as part of a museum collection. As a result, analysis was carried out on a flat surface prepared (as described below) on the rim of each coin. However, it was first necessary to evaluate whether metallographic analyses carried out on the prepared rim flats of the coins gave results, both compositions and microstructures, comparable with bulk characterizations obtained on the coin cross-sections. This evaluation was accomplished by examining both the prepared rim surfaces and the bulk cross-sections of four selected iron coins. Three of these were Song dynasty Chinese coins that were already in a damaged condition, so that it was permissible to cut bulk samples from them as well as to examine their rim surfaces, while the fourth was an 18th-century Japanese cast iron coin, then in a private collection and later donated to the Museum collection (Reg No 2000.1-5.1). For bulk analysis, two of these coins were sectioned completely across their cross-sections (from the outer rim to the central square hole) while wedge-shaped sections were cut inwards from the

Figure 1: Jiading tongbao coin. The front (left) has a four-character inscription 'Jia ding tong bao' arranged top-bottom-right-left around the square hole. 'Jiading' identifies the reign period, 'tong bao' means 'circulating treasure'. The back (right) has a two-character inscription 'chun er' arranged above and below the hole.

rims of the other two. Metallurgical analyses were then carried out on these cut sections and the results compared with the results of similar analyses carried out on prepared rim flats on the same coins.

After completing these preliminary investigations, which showed that the rim analyses were indeed sufficiently representative to be utilized with confidence, a further 34 coins were analysed, all on their rim surfaces.

To prepare an area on the rim for metallography, each coin was held in a purpose-built brass jig equipped with hard rubber padding to prevent gripping-damage. With the coin held firmly in the jig, a location on the rim of the coin was then abraded on silicon carbide grit paper using water lubrication and cooling. In most cases only a fine (600 grit) paper was used, however where necessary grinding started on coarser (240 or 320 grit) silicon carbide grinding paper and progressed through 400 grit to 600 grit with careful washing between stages. The grinding procedure produced a flat area a few millimetres in length across the full width of the coin rim.

With the coin still held in the jig, metallographic polishing of the flat area was then carried out on a polishing wheel rotating at 250 rpm, first using 6μm diamond paste on a nylon cloth and then 1μm diamond paste on a short-napped cloth, in both cases employing an oil-based lubricant. When the polished rim flat had been washed thoroughly and dried, the coin was removed from the jig and examined using a Zeiss reflected light microscope and a JEOL SEM which was equipped with an Oxford Isis EDX analysis system with a Ge detector and an ultra-thin detector window. Examination in this unetched condition provided information on the presence or absence of gas and shrinkage porosity, the state of corrosion damage, and the nonmetallic inclusion abundance and distribution. Also at this stage chemical microanalysis was carried out using SEM-EDX in order to determine the bulk contents of silicon, phosphorus, sulphur and manganese as well as the compositions of the nonmetallic inclusions. The polished flats were then etched with 2% nital and re-examined using both optical and scanning electron microscopy to characterize all of the microstructural constituent phases.

Standard reference materials were also analysed for silicon, phosphorus, sulphur and manganese by performing SEM-EDX analyses under conditions identical to those used for the coins. Those used were British Chemical Standards SS 551, SS 554 and 183/3, all issued by the Bureau of Analysed Samples Ltd, and NBS 661 from the US National Bureau of Standards. This confirmed that the lower limits of detection of these elements were approximately 0.1–0.15%. The SEM-EDX results can be considered to have a precision and accuracy of ±10–20% relative to the values obtained.

Carbon contents were estimated from photomicrographs of representative areas of the etched microstructures, as SEM-EDX is not suitable for carbon determination. The relative areas of proeutectic phases and eutectic constituents were obtained by point counting,and converted to carbon content by two methods. Assuming equilibrium cooling and using the equilibrium phase diagram gave one value for carbon content. However to allow for cooling being rapid enough that equilibrium conditions were not obtained, a second carbon content was calculated assuming that solidification occurred under equilibrium conditions but that no subsequent changes (other than the austenite-to-pearlite transformation),occurred during further cooling to room temperature. An estimated carbon content was obtained by averaging these two values, giving heavier weighting to the equilibrium value. The carbon contents thus obtained must be considered as accurate to no better than ±0.1% carbon.

Analytical results

Metallographic examination of the ground and polished rim flats showed that all of the coins have elemental compositions and microstructures that identify them unambiguously as white cast irons.

Compositions

The elements of major importance in determining the microstructures of cast irons are carbon, silicon, phosphorus, sulphur and manganese. The contents of the last four of these elements in the coins as determined using SEM-EDX are presented in Table 2. Detection limits for these elements are in the order of 0.1%, so concentrations less than this amount would not have been detected; these cases are reported in the Table as ‘nd’. The carbon contents were estimated as described above.

Silicon is present at detectable levels in some coins, with contents up to about 0.8% (Table 2). Microanalysis showed that the silicon is localized in the pearlite constituent of the microstructure, having been in solution in the austenite at high temperatures. The

phosphorus content also varies among the coins, up to a maximum of about 1.7% (note that this is very high by modern standards). The phosphorus is present in the microstructure as steadite, the binary or ternary eutectic constituent (*ie* the iron-iron phosphide eutectic mixture or the iron-iron phosphide-iron carbide eutectic mixture respectively).

The observed range of sulphur content as measured by SEM-EDX in these coins extends to slightly above 2%S, also far above levels in modern irons. Sulphur occurs in these cast irons in the form of sulphide inclusions in the microstructure; the sulphur contents in the iron matrix between the inclusions are below detection limits. The relative abundances of the sulphide particles as observed metallographically are in accord with the measured sulphur contents and correlate well with the two types of microstructure observed, ledeburitic

Table 2: Coin compositions and microstructures.

Coin	Reign period	Mint mark	Date range (AD)	Coin date (AD)	Si (wt%)	P (wt%)	S (wt%)	C (wt%)*	Mn (wt%)	Microstructure
cm7	Yuanfeng	-	1078-1085	-	0.32	0.60	0.90	3.4	nd	divorced eutectic
cm8	Yuanfeng	-	1086-1093	-	0.53	0.90	0.73	3.4	nd	divorced eutectic
cm9	Yuanfeng	-	1086-1093	-	0.70	1.38	1.06	3.1	nd	divorced eutectic
cm10	Zhenghe	-	1111-1117	-	0.71	0.79	1.71	2.6	nd	divorced eutectic
cm11	Zhenghe	-	1111-1117	-	0.20	0.30	0.15	3.1	0.31	mixed
cm12	Xuanhe	shaan	1119-1125	-	0.25	0.58	0.39	4.0	nd	divorced eutectic
cm13	Xuanhe	shaan	1119-1125	-	0.57	0.69	1.65	2.3	nd	divorced eutectic
cm17	Xuanhe	shaan	1119-1125	-	0.32	0.68	0.37	4.0	nd	divorced eutectic
cm14	Xuanhe	shaan	1119-1125	-	0.78	0.71	2.05	2.3	nd	divorced eutectic
cm15	Xuanhe	shaan	1119-1125	-	0.55	0.71	1.33	2.9	nd	divorced eutectic
cm16	Xuanhe	shaan	1119-1125	-	0.57	0.73	1.14	2.9	nd	divorced eutectic
cm18	Qiandao	-	1165-1173	-	0.18	1.35	0.41	4.2	nd	divorced eutectic
cm2	Chunxi	dot in crescent	1174-1189	1174-1179	0.25	1.48	1.97	2.6	nd	divorced eutectic
cm3	Chunxi	-	1174-1189	1174-1179	0.50	1.25	2.00	2.6	nd	divorced eutectic
cm19	Chunxi	dot in crescent	1174-1189	1174-1179	0.36	1.36	1.35	3.7	nd	divorced eutectic
cm20	Chunxi	-	1174-1189	1174-1179	0.25	1.65	1.52	3.4	nd	divorced eutectic
cm21	Chunxi	-	1174-1189	1174-1179	0.26	1.37	1.08	4.0	nd	divorced eutectic
cm30	Chunxi	chun	1174-1189	1174-1179	0.18	0.18	nd	4.3	nd	ledeburitic
cm33	Chunxi	tong	1174-1189	1174-1179	nd	0.14	nd	4.9	nd	ledeburitic
cm32	Chunxi	tong 12	1174-1189	1185	nd	nd	nd	4.0	nd	ledeburitic
cm31	Chunxi	chun 15	1174-1189	1188	nd	0.12	nd	4.3	nd	ledeburitic
cm34	Shaox	chun 1	1190-1194	1190	0.16	nd	nd	3.9	nd	ledeburitic
cm35	Shaoxi	chun 2	1190-1194	1191	nd	0.15	nd	4.2	nd	ledeburitic
cm36	Shaoxi	tong 2	1190-1194	1191	0.16	0.10	nd	4.0	nd	ledeburitic
cm37	Shaoxi	tong 5	1190-1194	1194	nd	nd	nd	4.3	nd	ledeburitic
cm6	Qingyuan	-	1195-1200	-	nd	0.31	nd	4.0	nd	ledeburitic
cm1	Qingyuan	-	1195-1200	-	0.13	0.13	nd	4.3	nd	ledeburitic
cm28	Jiading	han 1	1208-1224	1208	nd	0.22	nd	4.5	nd	ledeburitic
cm29	Jiading	han 2	1208-1224	1209	nd	0.16	nd	3.6	nd	ledeburitic
cm22	Jiading	chun 2	1208-1224	1209	0.10	0.18	nd	4.8	nd	ledeburitic
cm26	Jiading	tong 2	1208-1224	1209	nd	nd	nd	4.3	nd	ledeburitic
cm5	Jiading	3	1208-1224	1210	nd	0.25	nd	3.9	nd	ledeburitic
cm27	Jiading	tong 3	1208-1224	1210	nd	nd	nd	4.3	nd	ledeburitic
cm4	Jiading	chun3	1208-1224	1210	0.38	0.18	0.65	3.4	nd	mixed
cm23	Jiading	chun3	1208-1224	1210	0.14	0.12	nd	4.5	nd	ledeburitic
cm24	Jiading	chun4	1208-1224	1211	0.13	0.16	nd	4.8	nd	ledeburitic
cm25	Jiading	chun8	1208-1224	1215	0.13	nd	nd	3.9	nd	ledeburitic

Notes: nd = not detected; * carbon content estimated as described in text

and divorced eutectic, as will be discussed below.

Manganese was detected in only one of these coins (cm11) where the manganese content is about 0.3% and the sulphide inclusions were found to be mixed manganese-iron sulphides averaging more than 25%Mn. In all the other coins it must be present in amounts less than about 0.1%, its detection limit in the SEM-EDX system.

Other than in coin cm11, the sulphide inclusions are iron sulphides containing minor amounts of manganese (up to 5%) and titanium (up to 0.5%). However two of the coins, cm7 and cm12, also contain appreciable amounts of copper in some of the sulphide particles. These particular sulphide inclusions could be seen in the SEM to consist of two phases, the brighter of which contains as much as 20% copper. The sulphide particles in some of the other coins contain smaller (less than 1%) amounts of copper or vanadium.

Coin cm12 was observed to have a brassy colour, unlike any of the other coins, and XRF analysis showed that indeed a layer of brass containing approximately 70% copper and 30% zinc is present on the surface of this coin. The XRF spectrum exhibited strong iron peaks emanating from the base iron beneath the brass layer, showing that the brass layer is thin, likely of the order of a few tens of micrometres. Microscopical study of the surface of this particular coin showed that its topography is rough, as is usual in iron objects that have undergone surface corrosion, and that the brass layer is on the outer surface, *ie* on top of the corrosion layer. This was confirmed by examination of the edges of the ground and polished flat area of the coin rim, which revealed the brass layer in cross-section. These observations show that the brass layer must have been applied *after* the coin corroded, and so the brass layer must be unrelated to the original manufacture of the coin. The history of this particular coin is unknown, as it was an anonymous donation to the Museum. This is a very curious effect. It is conceivable that the brass layer could have been inadvertently deposited during electrochemical cleaning in an electrolyte containing copper and zinc ions, or possibly it was deliberately electroplated for unknown reasons. In any event this plating was certainly done in the relatively recent past, perhaps for collecting purposes. Song dynasty coins were still in use in the early 20th century.

Microstructures

No graphite was observed in any of the microstructures; the presence of graphite would have identified the materials as grey or mottled cast iron. Instead, although there were microstructural differences among the coins, all had white cast iron microstructures, *ie* mixtures of cementite and pearlite, with a range of morphologies as described below.

The details of the microstructures are given in Table 3, where it can be seen that the coins can be grouped into two major microstructural categories. One of these, termed 'ledeburitic', had a matrix of ledeburite (the eutectic constituent which consists of cementite and austenite, the latter typically having transformed to pearlite during cooling) with varying amounts of the proeutectic phases pearlite or cementite. Thus, for example, the microstructures of some coins contained only ledeburite (Fig 2), while others consisted of a matrix of ledeburite with various amounts of proeutectic pearlite (Figs 3 and 4) or proeutectic cementite (Fig 5).

Figure 2: Fully ledeburitic microstructure (cm31). Nital etch. Scale bar 50µm.

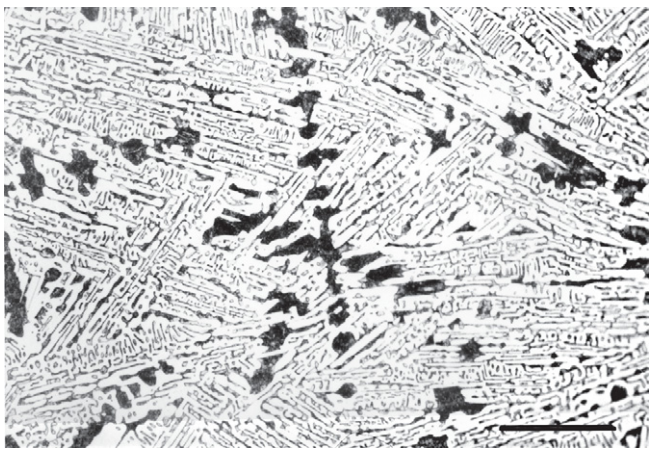

Figure 3: Microstructure of ledeburite with 10% proeutectic pearlite (cm32). The pearlite appears dark but close examination shows it to be lamellar ferrite and cementite. Nital etch. Scale bar 50µm.

Table 3: Details of coin microstructures.

Coin	Microstructure	Proeutectic phase	Steadite (phosphorus)	Sulphide inclusions	Gas porosity
cm1-R	ledeburite	none	very little*	few	micro
cm1-X	ledeburite with a few pearlite dendrites	pearlite (1%)	very little*	few	micro
cm2	divorced eutectic pearlite with cementite	pearlite (75%)	abundant*	abundant FeS	micro
cm3	divorced eutectic pearlite with cementite	pearlite (75%)	abundant*	abundant FeS	micro
cm4	divorced eutectic pearlite with cementite and minor ledeburite	pearlite (60%)	very little*	abundant FeS	micro
cm5	ledeburite with pearlite dendrites	pearlite (15%)	present*	few	micro & micro
cm6	ledeburite with pearlite dendrites	pearlite (10%)	present*	few	macro & micro
cm7	divorced eutectic pearlite with cementite	pearlite (60%)	present*	abundant FeS	macro & micro
cm8	divorced eutectic pearlite with cementite	pearlite (10%)	present*	abundant FeS	macro & micro
cm9	divorced eutectic pearlite with cementite	pearlite (65%)	present*	abundant FeS	micro
cm10	divorced eutectic pearlite with cementite	pearlite (75%)	present*	abundant FeS	micro & micro
cm11	ledeburite and cementite with pearlite dendrites	pearlite (40%)	present*	some FeMnS	macro & micro
cm12	divorced eutectic with pearlite dendrites	pearlite (50%)	present*	some FeS	macro & micro
cm13	divorced eutectic with pearlite dendrites	pearlite (80%)	abundant	some FeS	macro & micro
cm14	divorced eutectic with pearlite dendrites	pearlite (80%)	present*	abundant FeS	macro & micro
cm15	divorced eutectic with pearlite dendrites	pearlite (70%)	present*	abundant FeS	micro
cm16	divorced eutectic with pearlite dendrites	pearlite (70%)	present*	abundant FeS	micro
cm17	divorced eutectic with pearlite dendrites	pearlite (50%)	present*	some FeS	macro & micro
cm18	divorced eutectic with pearlite dendrites	pearlite (45%)	abundant*	some FeS	macro & micro
cm19	divorced eutectic with pearlite dendrites	pearlite (55%)	abundant*	abundant FeS	micro
cm20	divorced eutectic with pearlite dendrites	pearlite (60%)	abundant*	some FeS	micro
cm21	divorced eutectic with pearlite dendrites	pearlite (50%)	abundant*	some FeS	macro & micro
cm22	ledeburite with cementite laths	cementite (20%)	little or none	very few	macro & micro
cm23	ledeburite with cementite laths	cementite (9%)	little or none	very few	macro & micro
cm24	ledeburite with cementite laths	cementite (20%)	little or none	few	macro & micro
cm25	ledeburite with pearlite dendrites	pearlite (15%)	little or none	very few	micro
cm26	ledeburite with cementite laths	cementite (2%)	little or none	few if any	macro & micro
cm27	ledeburite	none	little or none	few if any	macro & micro
cm28	ledeburite with cementite laths	cementite (8%)	very little*	few	macro & micro
cm29	ledeburite with pearlite dendrites	pearlite (25%)	very little*	few	macro & micro
cm30	ledeburite with pearlite dendrites	pearlite (1%)	little or none	some FeS	macro & micro
cm31	ledeburite with cementite laths	cementite (1%)	little or none	few if any	macro & micro
cm32	ledeburite with pearlite dendrites	pearlite (10%)	little or none	tiny	macro & micro
cm33	ledeburite with cementite laths	cementite (26%)	little or none	few if any	macro & micro
cm34	ledeburite with pearlite dendrites	pearlite (15%)	little or none	few and tiny	micro
cm35	ledeburite with pearlite dendrites	pearlite (6%)	little or none	some FeS	macro & micro
cm36	ledeburite with pearlite dendrites	pearlite (10%)	little or none	few and tiny	macro & micro
cm37	ledeburite	none?	little or none	few and tiny	macro & micro

Notes: cm1, 4 and 5 were sectioned. In cm1 the rim (R) and cross-section (X) showed different microstructures, in cm4 and cm5 there were no differences.
* = on colony boundaries.

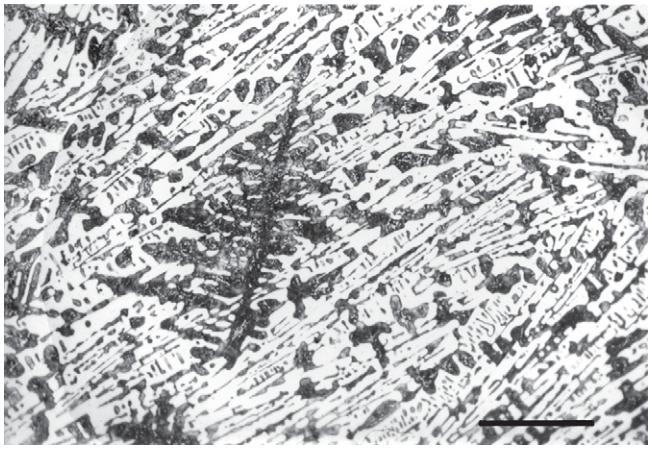

Figure 4: Microstructure of ledeburite with 25% proeutectic pearlite (cm29). Nital etch. Scale bar 50µm.

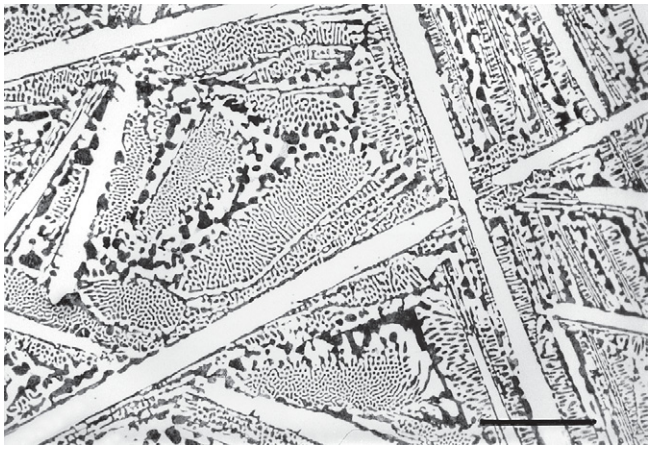

Figure 5: Microstructure of ledeburite with 20% proeutectic cementite in the form of laths (cm24). Nital etch. Scale bar 50µm.

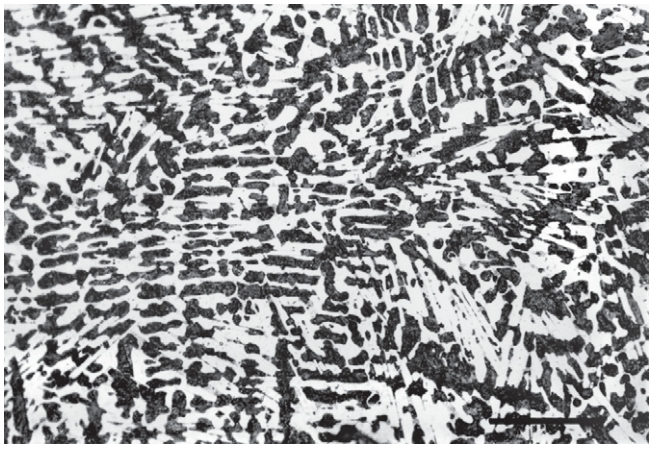

Figure 6: Divorced eutectic microstructure with 50% proeutectic pearlite dendrites in a cementite matrix (cm12). Nital etch. Scale bar 50µm.

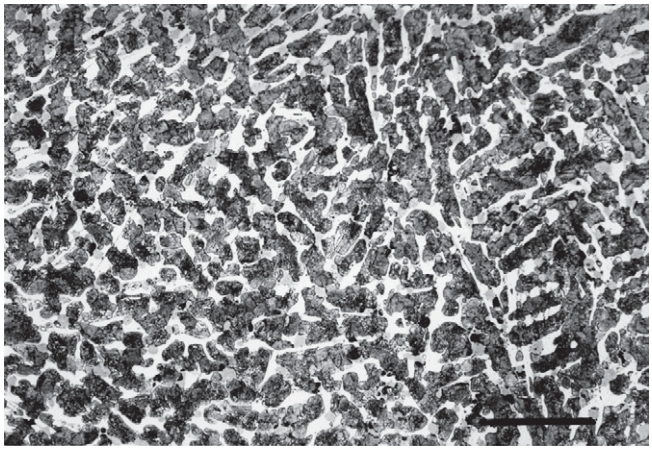

Figure 7: Divorced eutectic microstructure with 75% proeutectic pearlite dendrites in a cementite matrix (cm10). Nital etch. Scale bar 50µm.

This type of microstructure is typical of the solidification of eutectic and near-eutectic alloys, as described in the Discussion section below. The other type of microstructure observed, termed 'divorced eutectic', consisted of a matrix of cementite in which are embedded pearlite dendrites (Figs 6 and 7). In these coins the pearlite dendrites occupied between 45% and 80% of the microstructure, the balance being cementite. Two of the coins, cm4 and cm11, did not fall clearly into either group, as they had microstructures which were mixtures of the two main types.

In addition to the phases described above, several other microconstituents were observed to be present to varying extents within the microstructures of the coins (see Table 3). Notable among these are the phosphorus-bearing constituent steadite. Both the two- and three-phase eutectic mixture described above have melting temperatures below 1000°C and hence they are invariably found in the last regions of the microstructure to solidify, *ie* at the boundaries of the ledeburite colonies in the ledeburitic microstructures and between the proeutectic pearlite dendrites or ledeburite laths in the divorced eutectic microstructures. Steadite was observed in most of the coins; its relative abundance, as reported in Table 3, agreed well with the phosphorus contents of the coins as measured by EDX.

Another commonly observed microstructural constituent was inclusions of iron sulphide, some of which contained manganese as mentioned above. These sulphide particles (visible for example in Figure 7, where they appear as light grey blobs within the cementite) were found to be especially abundant in some coins and absent or extremely rare in others, as reported in Table 3.The observed abundances of sulphide inclusions in the microstructures were found to be higher in coins with higher measured sulphur contents (Table 2), as expected, and furthermore there is a striking correlation between sulphur content (or

sulphide particle abundance) and microstructural category. Thus the sulphur content in the ledeburitic coins was below detection limits, in sharp contrast to the levels in the divorced eutectic coins. Like the steadite, the sulphide particles are found at interdendritic locations since during solidification the sulphur, like the phosphorus, is concentrated in the liquid between the proeutectic constituents.

Along with the various metallurgical phases and constituents mentioned above, two types of porosity were observed in these coins, gas porosity and shrinkage porosity. Gas porosity, which occurs as spherical bubbles, arises when gases that are dissolved in the liquid iron are precipitated during solidification as a result of their having much smaller solubilities in solid iron than in the liquid. In contrast, shrinkage porosity is a consequence of the solid material occupying less volume than the liquid so that as the microstructural constituents grow together during solidification there is insufficient liquid metal available to form a space-filling metallic structure. The result is that gaps are left between the constituents, *ie* on the boundaries between the solidification colonies.

Gas porosity was observed to be present at a macroscopic scale in the form of spherical holes (Fig 8), many of which had become filled, or partially filled, with corrosion products. In addition, gas porosity on a finer scale (microporosity) occurred in most of the coins in the form of spherical holes about 1μm in diameter associated with the interdendritic constituents, typically the sulphide inclusions; some of this microporosity can be seen in Figure 7. Shrinkage porosity was present in all of the coins. In those coins that had ledeburite in the microstructure, the shrinkage porosity was manifest as gaps or irregular holes in the material at ledeburite colony boundaries (Fig 8).

X-radiography clearly revealed the macroscopic (0.1-1mm diameter) gas porosity in the form of small dark circular markings on the X-ray film (Fig 9). Some coins, notably cm37, displayed very considerable amounts of coarse gas porosity. The porosity in coin cm5 was so extensive in the region where its cross section was sampled that the coin appeared to be hollow; this was also visible in the radiograph. In this case the porosity was too great to be due to either shrinkage or gas, and is attributed to liquid metal feeding problems during the casting process, either because of poor mould gating system design, inadequate pouring temperature or some inadvertent restriction on metal flow into the mould.

Figure 8: Ledeburitic microstructure with proeutectic cementite, showing gas porosity (spherical voids) as well as shrinkage porosity (dark irregular voids between ledeburite colonies) (cm28). Nital etch. Scale bar 50µm.

Corrosion was also visible in most of the microstructures, having penetrated from the surface into the interiors of the coins (Fig 10), sometimes reaching or surpassing the midpoint of the cross-section. The pearlite constituent was attacked preferentially by the corrosion (*ie* pearlite was anodic in the corrosion reaction), so that the as-polished (*ie* unetched) surface of the corroded area showed surface relief with the cementite standing proud (the corrosion products having been spalled from the surface during grinding and polishing). Hence the microstructure could be clearly seen and identified in corroded areas even without etching. The corrosion of the pearlite, especially in the ledeburitic constituent, also created high stress

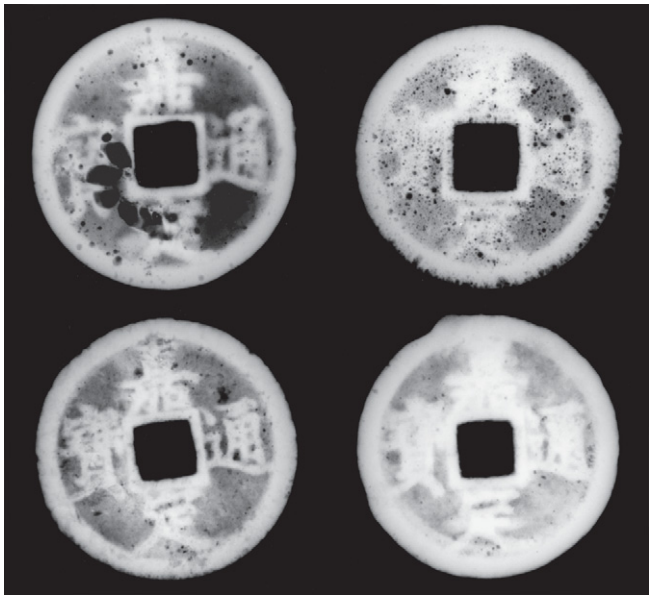

Figure 9: X-radiographs of four coins showing variable degrees of casting porosity. Clockwise from upper left cm26, cm27, cm29, cm28.

concentrations in the corroded area making the coins more susceptible to fracture, thus it was necessary to use extra care in handling the most heavily corroded coins. As corrosion progressed further, the cementite also corroded; at this stage the sulphide particles and sometimes traces of relict cementite could be discerned within the corrosion products. Where corrosion was severe no vestiges of the original microstructure remained.

Discussion

Early examples of cast iron, white, mottled or grey, are found only rarely outside China, and then usually either as apparently inadvertent products of bloomery furnace operation or as intermediate furnace products, *ie* pig iron intended for conversion into wrought iron. In China, however, cast iron tools and agricultural implements became common from about the mid-first

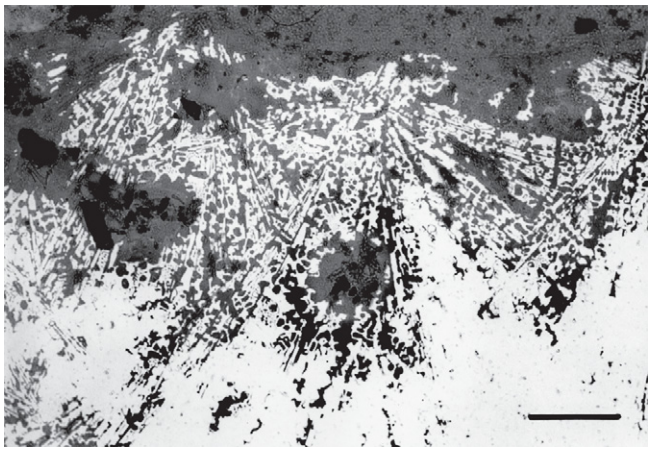

Figure 10: Corroded microstructure at the edge of a coin (cm11). The cementite remains white while the ferrite has corroded and now appears grey. Unetched. Scale bar 100µm.

millennium BC (Wagner 1993 and 1999, Bronson 1999). Chinese cast iron coinage appeared at least as early as the Han period, but only became commonplace between the 11th and 13th centuries AD. In some respects, white cast iron is an appropriate material for coins, at least for cast coins, since it is hard, has good wear resistance in the as-cast condition, and has acceptable casting properties, particularly when its phosphorus content is high. Furthermore, and most importantly, it is economically attractive, especially in comparison with other common coinage alloys such as bronze. Although white cast iron is a brittle material, the coins can be made with a thickness sufficient to keep applied stresses acceptably low, so that fracture in service should not normally be a problem. On the other hand white cast iron has comparatively high levels of solidification shrinkage, thus it reproduces mould features relatively poorly.

The elemental compositions of the coins reported in Table 2 were not unexpected. All of the analysed elements, in conjunction with cooling rate, play major roles in determining the characteristics of the cast iron. The coins displayed an appreciable range of carbon contents, from about 2.3% to 4.9%, close to the full range normally associated with cast irons. Significant variability was also found in the contents of silicon, phosphorus and sulphur in these coins, with maxima for the three elements at 0.78%Si, 1.65%P and 2.05%S. These compositions explain why all the observed microstructures were those of white cast iron. At similar cooling rates, white cast iron is formed in irons that have low values of Si and C and high values of S. None of the coins fell into a composition range where grey cast iron would have been expected. For example, iron containing carbon above 3%, silicon above 1% and sulphur below 0.1% would be expected to solidify as grey cast iron, but none of these coins came close to such a composition; none had silicon contents high enough to cause the formation of grey cast iron, and those with even moderate silicon contents also contained sufficient sulphur to more than compensate for the silicon. Their compositions suggest that even at unrealistically slow cooling rates it is highly unlikely that any of these coins would have solidified as grey cast iron.

It is clear from Table 2 that in a general way the coins could be divided into two groups, one group of 17 coins having more than 1.2% total (P+Si+S) and the other group of 20 coins having less than 0.7% total (P+Si+S). In addition, although there was a slight overlap, the carbon contents of the two groups were also different, with the first group having an average carbon content lower than that of the second. This inverse relationship with carbon content is not unexpected because silicon, phosphorus and sulphur all lower the solubility of carbon in liquid iron.

The grouping of the coins based on elemental composition, as described in the preceding paragraph, was found to correspond almost exactly with the two groups based on microstructures. All of the 19 coins with total (P+Si+S) contents below 0.5% had ledeburitic microstructures, while the 16 coins with high values of (P+Si+S) content all had divorced eutectic microstructures. The two coins that were observed to have mixed microstructures, *ie* ledeburite together with divorced eutectic, were intermediate

between the two groups on the basis of elemental composition as well as on the basis of microstructure. The origins of these types of microstructure will now be explained and then the two coin groups can be discussed further.

Explanation of observed microstructures

The microstructural characteristics of the Song coins can be explained with reference to the Fe–Fe_3C equilibrium phase diagram (Fig 11). According to this diagram, when a molten iron-carbon alloy containing 4.3% carbon (the eutectic composition) solidifies under equilibrium (slow) cooling conditions it should transform at the eutectic temperature, 1150°C, to a two-phase eutectic mixture of cementite (Fe_3C) and austenite (γ-iron) known as ledeburite. Ledeburite is not strictly lamellar, as are many eutectic microconstituents, but rather it consists of plates of cementite interspersed with branched linear arrays of austenite whose branches often run at high angles to the direction of growth of the ledeburite colony. Furthermore these branches do not fill the entire space between the cementite plates, but some cementite infill forms along with the austenite branches, resulting in the distinctive ledeburite morphology. On continued slow cooling, the solid austenite rejects carbon, so that the amount of cementite

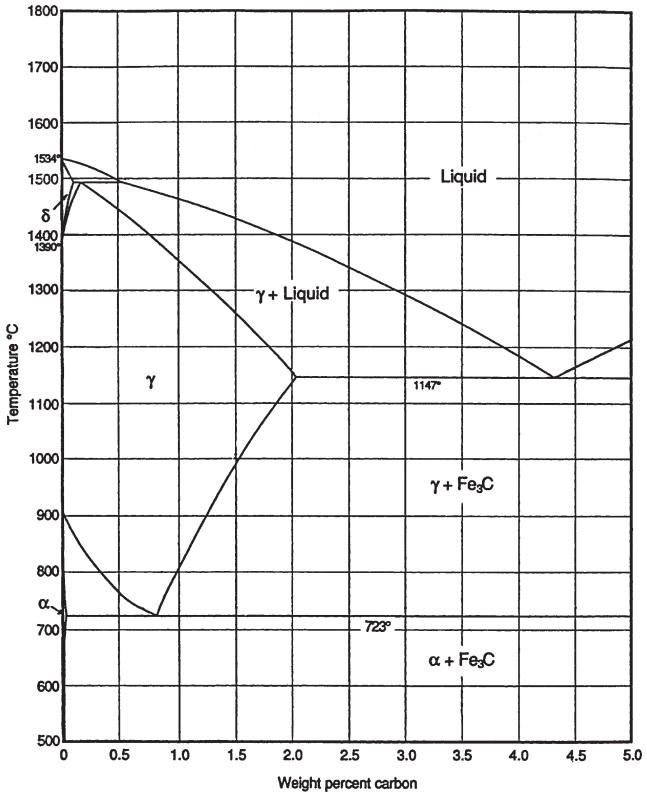

Figure 11: Iron-iron carbide (cementite) metastable phase diagram; adapted from Hansen & Anderko 1958, 354.

increases, via the growth of pre-existing cementite as well as, possibly, the precipitation of cementite plates within austenite grains. On cooling through the eutectoid temperature (725°C) the remaining austenite transforms to pearlite, creating the final microstructure since no further changes are expected during further cooling to ambient temperature. This is the simplest form of the microstructure referred to here as ledeburitic, which is exemplified by Figure 2.

Cooling of liquid cast irons with carbon slightly below the eutectic composition causes the formation of proeutectic austenite dendrites in the liquid, with the remaining liquid transforming to ledeburite as described above when the eutectic temperature is reached. Subsequent cooling towards 725°C under equilibrium conditions then causes the rejection of carbon by the austenite, and thus an increase in the amount of cementite as described above. After the remaining austenite transforms to pearlite at 725°C, the final microstructure consists of pearlite dendrites in a background matrix of ledeburite. The microstructures of coins with lower carbon contents would exhibit larger amounts of proeutectic dendrites in a ledeburite matrix as shown in Figures 3 and 4. Coins with slightly more than the eutectic carbon content would solidify in the same way except that the proeutectic phase would be cementite, which is present as plates rather than dendrites as shown in Figure 5. This provides an explanation for the observed microstructures of the ledeburitic group of coins.

The description of solidification outlined in the previous paragraphs is normal for alloy systems, but another possibility exists, the formation of so-called 'divorced eutectic' microstructures. These are more likely to form at compositions well above or well below the eutectic composition, and are encouraged by slower cooling rates. In the solidification of white cast irons with well below 4.3%C, the phase diagram (Fig 11) predicts that significant amounts of proeutectic austenite dendrites will form in the liquid so that when the eutectic temperature is reached a relatively small amount of liquid remains between these dendrites. At the eutectic temperature this eutectic liquid freezes, but rather than this happening by the formation of austenite and cementite in the form of ledeburite, the austenite phase of the eutectic solidifies on the pre-existing austenite dendrites, causing them to grow, while the eutectic cementite precipitates in the interdendritic spaces. Hence instead of obtaining the intimately intergrown austenite and cementite mixture of phases (ledeburite), the austenite and cementite form separately (*ie* 'divorced' from each other).

As in the ledeburitic coins, subsequent cooling under equilibrium conditions from the eutectic temperature down to the eutectoid temperature (725°C) would be expected to cause some of the austenite to transform to cementite, hence the cementite in the interdendritic spaces would be expected to grow. This was observed, with significant amounts of cementite plates being present. At the eutectoid temperature, the remaining austenite transforms to pearlite, resulting in the microstructures observed (Figs 6 and 7).

Although not observed in any of the coins examined here, divorced eutectic microstructures can also form at hypereutectic compositions. In this case solidification occurs by the formation of proeutectic cementite plates, with the eutectic constituents again forming separately at the eutectic temperature. In this case the eutectic cementite forms on the proeutectic plates, causing their growth, and also as interdendritic laths. At the same time the austenite forms in the interdendritic spaces but not coupled with the cementite, as it is in ledeburite. Again the austenite transforms to pearlite on subsequent cooling, so that the final microstructure is a matrix of pearlite enclosing cementite plates. Examples of this process, hypereutectic white cast irons with divorced eutectic microstructures (*ie* with proeutectic cementite), have been observed in other ancient Chinese cast irons (*eg* Wayman *et al* forthcoming).

Discussion of microstructures

With this background, the observed coin microstructures can be considered in more detail. Clearly the elemental compositions will have been important in determining the microstructures, and in fact a causal relationship can be seen to exist between the elemental compositions of the coins and their type of microstructure, *ie* ledeburitic *v* divorced eutectics. As described above, divorced eutectics are more likely to form when the amount of proeutectic phase is large, *ie* when the carbon content is far below or far above the eutectic. This was in fact observed, as the average carbon content of the divorced eutectic coins (Table 2) was found to be 3.2%, whereas the average for the ledeburitic coins was 4.2%. However, it is apparent from Table 2 that there were a few exceptions to this trend, with several coins exhibiting divorced eutectic microstructures despite having carbon contents which were relatively high (relatively close to the eutectic composition), in conflict with expectation. The determining factor in these cases is likely to be their high phosphorus contents, as phosphorus is known to stimulate divorced eutectic microstructures in hypoeutectic white cast irons such as these (Bailey and Samuels 1971, 129). The coins with divorced eutectic microstructures were all observed to have phosphorus contents above 0.58%. It is of interest in this regard to consider the microstructures of coins having the same carbon content but different phosphorus contents. Here again the results support the role of phosphorus in stimulating the divorced eutectic microstructures. For example, cm12 and cm25 both have nearly the same carbon contents however the higher phosphorus coin (cm12: 0.58%P) has a divorced eutectic microstructure while cm25, with its low (less than the detection limit) phosphorus content is ledeburitic.

The effects of the sulphur and silicon contents on the formation of divorced eutectic microstructures in cast iron do not seem to have been reported in the literature, because both of these elements were present in the coins at levels well above the ranges exhibited by modern cast irons. It is certainly possible that one or both of these elements could complement the carbon content in stimulating the formation of the divorced eutectic. The correlation between high sulphur content and a divorced eutectic microstructure (Table 2) is particularly striking, with the ledeburitic microstructures having a maximum of 0.31%S and the divorced eutectics a minimum of 0.37%S (again with the exception of the mixed-microstructure coin cm11, discussed below). It is possible that along with the lower carbon and higher phosphorus contents, the higher levels of sulphur could be a factor in the development of divorced eutectic microstructures. A similar effect was noted in a group of Chinese white cast iron statuary dating from the 9th to the 19th centuries AD (Wayman *et al* forthcoming).

Two of the coins exhibited microstructures that included both ledeburite and divorced eutectic components, being in a transition state between the two microstructural groups. One of these, coin cm11, had a ledeburitic microstructure which was not as clearly defined as the other ledeburitic structures, its appearance suggesting that it was close to the transition between ledeburite and a divorced eutectic. This is consistent with its composition, as its carbon content was low compared to the other ledeburitic coins, while its silicon, phosphorus and especially sulphur contents were low compared to the other divorced eutectic coins. The case of coin cm4 was comparable in that it was mainly a divorced eutectic but contained a small amount of ledeburite, consistent with its combination of relatively high carbon, relatively low phosphorus and relatively high sulphur.

Few analyses have been reported on other Chinese cast

irons of similar or earlier date (see, *eg* Pinel *et al* 1938, Henger 1970, Rostoker *et al* 1984, Wagner 2000 and tabulated data from Chinese sources in Rostoker and Bronson 1990, tables 10.3–10.4, Wagner 1993, table 7.1 and Bronson 1999, table 7.4), but those which do exist compare well with the compositions and microstructures of these coins. Furthermore, work currently in progress (Wayman *et al* forthcoming) is yielding results that are also in accord with these.

Smelting conditions

It is of interest to consider the extent to which the characteristics of these coins can be interpreted to yield information about the iron smelting technology. One important aspect is the question of whether the iron in these coins was smelted using coal or coke as opposed to charcoal to provide the high temperatures and reducing atmospheres needed for blast furnace operation. Although the use of mineral fuels in iron smelting was not successfully achieved in Europe until the early 18th century AD, it is clear that coal or coke was being used for smelting iron in Song times, and there are suggestions of much earlier use (see, *eg* Read 1939–40, Hartwell 1966, 55 and 1967b, 118, Till and Swart 1993, 40, Golas 1999, 196 and Wagner 2001).

Wagner (2001 and pp 25–77 below) has given direct consideration to the dates at which coal or coke came into relatively widespread use in iron smelting, based to some extent on early writings but also quoting the results of scientific examinations by others. He quotes a text reference from the 4th century AD which seems to refer to the use of coal in iron smelting, though it is important to note that the use of coal or coke in metallurgy for purposes such as heating of annealing furnaces or baking moulds may well have preceded their use in blast furnaces by many centuries (*eg* Han Rubin 1996,152). Wagner also points out that very many such references suddenly appeared in writings of Song times. Since this was a time of serious wood shortage (*eg* Hartwell 1967b), an increased emphasis on the use of mineral fuel is not surprising. On the question of which of the mineral fuels, coal or coke, was being used, Wagner points out that coke has been used in China since very early times, and Hartwell (1963, 69–70 and 1966, 55–57) and Golas (1999, 196) refer to the specific use of coke in iron smelting during the Song period.

The scientific evidence for the use of coal or coke referred to by Wagner (2001) includes three radiocarbon analyses obtained by Qiu Shihua and Cai Lianzhen (1986) from Song/Yuan cast iron objects which gave dates ranging between 11,500 and 14,000 years BP. Wagner notes that these are far too early to be possible valid dates *per se*, and suggests that they could result from a mix of charcoal and coke/coal in the smelting furnace, although such mixed fuels are not otherwise attested. Alternative explanations for these dates without invoking the use of mineral fuel include the use of a carbonate mineral such as limestone in the flux, or possibly the use of iron carbonate ore (the carbon present in coal and in carbonates are both infinitely old from a radiocarbon perspective). However the most likely explanation for the dates is that the objects could have been cast from a second furnace in which charcoal smelted iron and coal/coke smelted iron had been remelted together. It is becoming more evident that attempts to apply radiocarbon dating to the carbon present in ferrous materials have the potential to yield erroneous results for a variety of reasons (Craddock *et al*, in press)

The other scientific evidence for the use of coal or coke referred to by Wagner (2001) is the presence of sulphur in cast iron artefacts. Many coals contain appreciable amounts of sulphur, most of which remains after its transformation to coke, whereas charcoal contains little or no sulphur. The smelting conditions in early blast furnaces are likely to cause the majority of this sulphur to end up in the cast iron. The most simplistic approach would therefore be to say that high sulphur content in the cast iron can be identified with a coal- or coke-burning blast furnace, whereas low sulphur content is indicative of charcoal smelted iron. This argument has been used frequently, for example by Rostoker and Bronson (1990) and also by Han Rubin (1996, 154) who interprets a positive response to a sulphur print as evidence for the use of coal.

Unfortunately, this type of argument is complicated by a number of other factors. One is that sulphur is also a constituent of some iron ores, in the form of the mineral pyrite (iron sulphide) that could contribute sulphur to the cast iron even if the iron was charcoal-smelted, although roasting of the ore prior to smelting is likely to drive off most of this sulphur. Another factor, probably of more importance, is that some coals have intrinsically low sulphur contents, so that iron smelted with these coals would not acquire high levels of sulphur. For example, if coal or coke use results in higher smelting temperatures (see below), more sulphur can be transferred to the slag phase, especially if limestone is used as a flux. This would be expected to give a sulphur level lower than in iron smelted with coke at lower temperatures, however still higher than

in charcoal-smelted iron. For these reasons it cannot be said with absolute confidence that a high sulphur content in the iron is proof that the iron was smelted with coal (coke) or that low sulphur iron comes from smelting with charcoal.

However, a review of the results of previously reported chemical analyses of charcoal- and coke-smelted cast irons from early (pre-4th century AD) China and from early European blast furnace products (Evrard and Descy 1948, Henger 1970, Tylecote 1976 and 1991, Pfannenschmidt 1977, Rostoker and Bronson 1990, Wagner 1993, Bronson 1999) shows that although charcoal-smelted iron almost always displays low sulphur contents, *ie* below 0.1%S, and coke-smelted irons are normally well above 0.1%S, some coke-smelted cast irons do display low sulphur levels, as low as 0.05%S. On the other hand, of all of the charcoal-smelted cast irons analysed, none had sulphur levels much above 0.1% and only one was above 0.2%S, which confirms that the use of high-sulphur iron ore was not common. Thus the empirical evidence is that although a low sulphur content cannot be considered as absolute proof of the use of charcoal in iron smelting, a high sulphur content is in fact strongly indicative of the use of mineral fuel, *ie* coal or coke.

Discussion of composition

The question of furnace temperature is one that can be addressed by considering the results of the coin analyses since high silicon and manganese contents of cast iron are potential indicators of high furnace temperature. Silicon enters the iron-smelting furnace in the gangue (waste) material associated with the ore minerals, as well as being a constituent of the furnace-lining materials. The gangue, along with reacted furnace linings and fuel ash, becomes the smelting slag, and silicon partitions between metal and slag, with more silicon reduced into the metal at higher smelting temperatures. Once again, the choice of fuel plays a role. Since coal- or coke-fired furnaces can be expected to operate at higher temperatures than charcoal-fired furnaces (*eg* Rehder 1987), the argument could be made that high-silicon cast irons are more likely to have been coal- or coke-smelted. However, many variables other than the fuel are involved in determining furnace temperature, notably furnace size and air blowing rate. Charcoal-fired blast furnaces can in fact be operated under conditions such that they achieve temperatures high enough to produce high-silicon cast iron.

It is of course a reasonable possibility that the iron used to make some of the coins was coke-smelted while other coins were made of charcoal-smelted iron. (In the Japanese coin analysed in the preliminary work, the iron, which was undoubtedly the product of a charcoal-fired furnace, was found to have low sulphur content). As iron smelting using coal or coke was becoming much more common during the Song dynasty, the time when these particular coins were produced, it could be expected that both charcoal- and coal/coke-fired furnaces might have been in use at the same time, possibly even in the same geographic region at the same time. Furthermore, it is not impossible that some smelting furnaces were fired using mixtures of charcoal with coal or coke, and it is even more likely that in many if not all cases the coins were cast from remelting furnaces where coal-smelted and coke-smelted irons could have been mixed. Consequently, the wide range of silicon and sulphur contents observed in the coins is not surprising.

The other elements of interest are carbon, phosphorus and manganese. Carbon is reduced from the charcoal or coal (coke), and higher furnace temperatures along with more strongly reducing conditions are expected to yield a higher carbon content in the iron product if no other variables are considered. However higher furnace temperatures reduce more silicon and phosphorus into the iron, and these lower the carbon content of the liquid iron. In line with this, the coins with higher silicon and phosphorus contents were found in general to have slightly lower carbon contents than the low silicon-phosphorus coins. Phosphorus in cast iron normally originates in the iron ore, where phosphorus-bearing minerals are present along with the iron-bearing minerals. During smelting, the phosphorus dissolves in both the metallic iron and the silicate smelting slag but in general most of the phosphorus is expected to enter the metal. The variability of the phosphorus content in the coins presumably reflects some combination of higher furnace temperatures and the use of different iron ores, although slag conditions also affect the partition.

The higher furnace temperature would also be expected to reduce some manganese into the iron, provided that manganese is present in the ore, and hence the absence of detectable manganese in most of these coins suggests that low-manganese ores were smelted and/or that smelting temperatures were low. The iron in the one coin with a detectable manganese content, cm11, is likely to have been smelted from a different ore in comparison with the other coins; its silicon content was too low to be indicative of a high smelting temperature.

Another question which remains unanswered is whether the coins were cast into the coin moulds directly from a smelting (blast) furnace or from a remelting (*eg* cupola-type) furnace where iron, possibly iron that had originally been smelted in different furnaces and now in the form of pig iron and/or scrap, was melted together. Information obtained from these analyses does not shed light on this question. Although casting conditions can be better controlled from a remelting furnace, casting directly from a blast furnace has long been a common technique, for example most post-medieval European cast iron cannon were cast in this manner (Rostoker 1986). On the other hand, during Song times at least some iron used for coins was smelted elsewhere than at the mint sites, for example locally in payment of taxes, and delivered to the mint sites (Hartwell 1962) where it would necessarily have been remelted for casting into coins.

Geographical and chronological differences

With the above thoughts in mind, it is of interest to consider the geographical origins of the Song coins analysed in this study. Mint locations are known for 23 of the 37 coins (Table 4). On the basis of the mint marks, six of the 23 coins were minted in modern-day Shaanxi province, north-central China, while the other 17 were minted in different mints: at Qichun (nine coins); Tong'an (six coins); and Hanyang (two coins). These

Table 4: Coins with mint marks.

Coin	Reign period	Coin date (AD)	Si (wt%)	P (wt%)	S (wt%)	C (wt%)*	Microstructure
Shaanxi							
cm12	Xuanhe	1119-1125	0.25	0.58	0.39	4.0	divorced eutectic
cm13	Xuanhe	1119-1125	0.57	0.69	1.65	2.3	divorced eutectic
cm17	Xuanhe	1119-1125	0.32	0.68	0.37	4.0	divorced eutectic
cm14	Xuanhe	1119-1125	0.78	0.71	2.05	2.3	divorced eutectic
cm15	Xuanhe	1119-1125	0.55	0.71	1.33	2.9	divorced eutectic
cm16	Xuanhe	1119-1125	0.57	0.73	1.14	2.9	divorced eutectic
Qichun Inspectorate, Qizhou							
cm30	Chunxi	1174-1179	0.18	0.18	nd	4.3	ledeburitic
cm31	Chunxi	1188	nd	0.12	nd	4.3	ledeburitic
cm34	Shaox	1190	0.16	nd	nd	3.9	ledeburitic
cm35	Shaoxi	1191	nd	0.15	nd	4.2	ledeburitic
cm4	Jiading	1210	0.38	0.18	0.65	3.4	mixed
cm22	Jiading	1209	0.10	0.18	nd	4.8	ledeburitic
cm23	Jiading	1210	0.14	0.12	nd	4.5	ledeburitic
cm24	Jiading	1211	0.13	0.16	nd	4.8	ledeburitic
cm25	Jiading	1215	0.13	nd	nd	3.9	ledeburitic
Tong an Inspectorate, Shuzhou							
cm33	Chunxi	1174-1179	nd	0.14	nd	4.9	ledeburitic
cm32	Chunxi	1185	nd	nd	nd	4.0	ledeburitic
cm36	Shaoxi	1191	0.16	0.10	nd	4.0	ledeburitic
cm37	Shaoxi	1194	nd	nd	nd	4.3	ledeburitic
cm26	Jiading	1209	nd	nd	nd	4.3	ledeburitic
cm27	Jiading	1210	nd	nd	nd	4.3	ledeburitic
Hanyang Inspectorate							
cm28	Jiading	1208	nd	0.22	nd	4.5	ledeburitic
cm29	Jiading	1209	nd	0.16	nd	3.6	ledeburitic
Dot in Crescent							
cm2	Chunxi	1174-1179	0.25	1.48	1.97	2.6	divorced eutectic
cm19	Chunxi	1174-1179	0.36	1.36	1.35	3.7	divorced eutectic

Notes: nd = not detected; * = estimated, as described in text

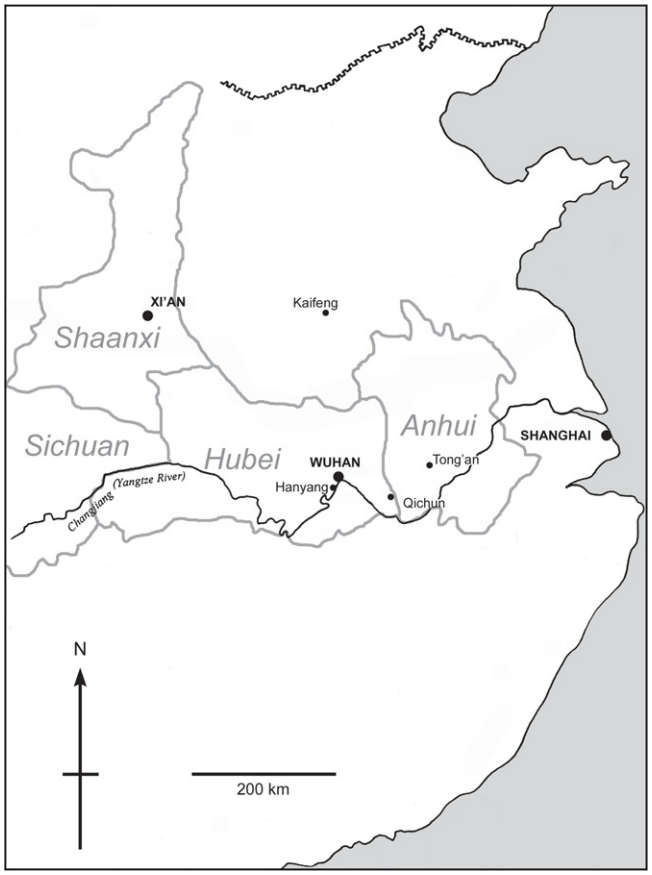

Figure 12: Map of central China showing the locations of the mints discussed, with names of present-day cities in upper case.

three named mints were in the Song administrative departments of Qizhou, Shuzhou and Ezhou, respectively, and are located in modern-day Hubei and Anhui provinces, about 1000km to the southeast of Shaanxi (Fig 12). These two different locations correspond with the two main areas where iron coins were circulated: Sichuan/Shaanxi and the Hubei/Anhui region, respectively.

Recent work relating to Song dynasty coins indicates that Qichun was close to modern-day Qichun, Hubei; Tong'an to modern-day Shucheng, Anhui; and Hanyang to modern-day Wuhan, Hubei. Combining historical texts and archaeological finds, Chen Hao (2002) writes that the Qichun mint opened in 1170, was expanded in 1185, and closed *c*1236–37. Annual production reached 200,000 strings in 1185. The Hanyang mint opened *c*1190, and closed after 1232 (its annual production was reckoned together with the Fumin mint, at 200,000 strings in 1212). The Tong'an mint has recently been excavated (Jin *et al* 2000), and among the finds were remains of poured iron as well as finished and unfinished iron coins of the Daguan (1107–1110) and Zhenghe (1111–1118) periods. This mint is known from historical records to have been casting iron coins during the period 1099–1214 (Jin *et al* 2000). The Tong'an coins analysed here are all from the final 30 years of production. Two Chinese publications on Song dynasty iron coins (Liu Sen 1997 and Yan Fushan 2001) should provide further details of these and other mints; for further reference to the Shaanxi mints, see Wang Shengduo 1998.

It is significant that in terms of composition and microstructure the Shaanxi coins are all similar to each other, being of the type which has high impurity levels and divorced eutectic microstructure, whereas all of the Hubei/Anhui coins are also similar to each other but of the other type, with low impurity contents and ledeburitic microstructures. This suggests that the three Hubei/Anhui mints were using the same or similar ore, the same or similar smelting conditions and that at least some of these parameters were different in the smelters that provided the Shaanxi mint. It is suggested that the difference between the Shaanxi coins and the Hubei/Anhui coins may well be related to the choice of smelting fuel in the different geographical locations, *ie* coal or coke in Shaanxi and charcoal in the Hubei/Anhui region. Coal deposits are concentrated in the more northerly regions of China, including Shaanxi and in Sichuan, and it is known that coal production underwent explosive growth during the Song dynasty, stimulated by a shortage of wood on the north China plain (Golas 1999). On the other hand the south was much more heavily wooded, and the easy availability of wood meant that charcoal was greatly preferred as a fuel there. It is of interest to note that during the Northern Song period, serious shortages of charcoal in Kaifeng, the Song capital, necessitated the import of charcoal from the south, and a gradual change to coal or coke as a domestic fuel (Hartwell 1967b). These considerations are fully consistent with the suggestion that the iron used for the Shaanxi coins was smelted with coke and that for the Hubei/Anhui coins with charcoal.

If the coins are considered strictly chronologically, all of the earlier (1078–1125 AD) ones have higher impurity contents and divorced eutectic microstructures, whereas the later (1174–1215 AD) coins, other than those minted during the Chunxi reign period (1174–1189), were of the low impurity, ledeburitic type. Of the nine analysed Chunxi period coins, five were in the earlier group and four in the later group. However, of the coins for which mint locations are known, all of the Shaanxi coins are early whereas all of the Hubei/Anhui coins are late, hence it is not possible to separate the effects of geographical location from

those of chronology. Furthermore, it must be noted that the time interval between the earlier and later coins is relatively short, a matter of some 50 years. In view of the number of coins analysed here, it does not seem reasonable to draw firm conclusions with respect to the changes over time.

In summary, it can be said that there are great similarities among the coins minted within each of the two geographic regions, but very significant differences between the coins from the two regions. The sulphur contents of the Hubei/Anhui coins are so low as to suggest strongly that they are made of charcoal-smelted iron. The Shaanxi coins have undoubtedly been smelted from a different ore, but their higher silicon contents suggest higher smelting temperatures, and this in combination with the observed higher sulphur levels suggest strongly that they are likely to have been made of coke-smelted iron.

Coin production and processing

Examination of the microstructures revealed that all of the coins were in the as-cast condition, with no indications that following the casting operations the coins had been subjected to any thermal processing. This is as expected; there is no obvious reason why such heat treatment would be desirable. In the mid-first millennium BC, Chinese ironworkers learned to heat treat white cast iron in order to decompose the cementite and then precipitate it as agglomerations of graphite, making malleable cast iron (Wagner 1989), a process that much improved the toughness of the material (this malleablizing heat treatment did not appear in Europe until the late 17th century AD). Alternatively the heat treatment could remove the carbon from the cast iron without the precipitation of graphite, transforming it into a form of wrought iron or, in some cases, steel. Both of these heat treatments would have degraded the service performance of the coins, and it is not surprising that they were not used.

Some of the coins examined here showed evidence of the casting process by which they were produced, in the form of stubs projecting from the outer rim. These are vestiges of the gating system (sprues and ingates), the channels through which molten iron flowed in to fill the moulds. Because white cast iron is so hard and resistant to deformation, removal of these projections would have been very difficult to accomplish; filing or sawing would not have been possible for example. The hardness and strength of the white cast iron would also have precluded mechanical working, for example by forging or stamping, and, not surprisingly, no evidence of mechanical working was visible in the microstructures of the coins.

Since the coins were produced in large numbers (Peng Xinwei 1965) they would certainly have been cast using a high volume production process. It is likely that they were cast in 'trees', complex moulds in which many coins could be cast simultaneously from a central gating system, creating a solid array of branches (the frozen ingates) with a cast coin at the end of each branch (Burger 1976). This type of production technique would have been necessary to produce coins at the high rates and volumes required. Bronze coins were often cast directly in bronze moulds, many of which have been found. The moulds for the iron coins could also have been made of metal (permanent moulds) which would likely have survived hundreds of refillings before degrading to the point where they would have had to be replaced (Rostoker *et al* 1983). As an alternative to metal moulds, tree-type clay or sand moulds could have been utilized. Burger (1976) describes the process used for bronze coins. This process starts with 'mother' coins that served as patterns, and involves pressing the mother coins into a mould material such as a mixture of earth (loam) and coal to produce a mould, assembling a number of moulds into a stack and then pouring the casting. Here the mould would be destroyed with each casting, and mould production would be a major part of the casting operation. That the Chinese used this technique for casting bronze coins is well documented (*eg* Burger 1976 and Williams 1997, 141) and it is likely to have been used for iron coins as well. A related high volume stack moulding system was extensively used for production of iron castings for agricultural tools, hardware, etc. (Rostoker *et al* 1983, Hua Jue-ming 1983, Li Jinghua 1996), with both metal and clay moulds being employed. The recent report of the excavation of the Tong'an mint site (Jin *et al* 2000) did not mention mould material being found, but did mention pot sherds, porcelain sherds and broken brick from the Song period level. After casting, clay coin moulds must be broken open to remove the cast coins, leaving only fragments that could have appeared similar to, and be mistaken for, pot sherds.

The coin microstructures, which have the potential to provide information about cooling rates of the liquid metal during and after freezing, were not revealing in this respect; none of the coins exhibited a chilled surface microstructure of the type which would be expected from rapid cooling. Rapid cooling is normally associated with metal moulds, which have good heat

transfer and heat absorption capabilities. However rapid cooling can create problems when casting a small object like a coin, or especially an array of coins cast simultaneously. In these situations it is important to have enough metal flow to fill the mould(s) completely, avoiding premature freezing in the gating system which would block subsequent metal flow. In the case of white cast iron this is a particularly serious problem, more serious than for bronze coins, because the ingates must be relatively slender so that the coins can be readily broken off the 'trees' after solidification (the extreme hardness of white cast iron limits the possible techniques for this detachment). One way to use a metal mould with constricted ingates while avoiding their being blocked by premature freezing, would be to preheat it prior to casting in order to slow the cooling rate. With such preheating, a chilled surface on the coins would not have been expected even if metal moulds had been used. Furthermore, the temperature of the liquid iron prior to casting plays a role in determining cooling rate independently of mould material. Hence it is not surprising that the microstructure of the coin was unable to help determine the material from which the moulds had been made.

Conclusions

All the 37 coins analysed were found to have been made of white cast iron. Based on their compositions, the coins fell into two groups, one with relatively high levels of silicon, phosphorus and sulphur and relatively low carbon contents and the other with relatively low levels of silicon, phosphorus and sulphur and higher carbon contents. These compositional groupings are fully consistent with their microstructures which also fell into two groups, divorced eutectic microstructures in the high impurity low carbon irons, and ledeburitic microstructures in the low impurity high carbon irons. Two coins are intermediate between these two groups, both in composition and in microstructure. The fact that all of the coins are white cast irons is fully consistent with their compositions as they have relatively low silicon contents and many have relatively high levels of sulphur.

Of the 23 coins whose geographical origins are known from mint marks, two general minting areas are represented. Coins minted in Shaanxi were found to be all similar and of the divorced eutectic type. These are quite different from the coins minted in Hubei and Anhui, about 1000km to the southeast, which are again similar to each other but different from the Shaanxi coins, being of the ledeburitic type. Although it is not possible to be certain, the cast iron from the Hubei/Anhui region is likely to have been smelted in charcoal-fired blast furnaces, while the iron in the Shaanxi coins is likely to have come from coke-fired blast furnaces. The coins were found to be in the as-cast condition, with no evidence of subsequent heat treating or working.

Acknowledgements

The authors are grateful to Dr P T Craddock for initiating this project and for support and discussion throughout. They also acknowledge with gratitude the helpful comments of Dr D B Wagner.

References

Bailey A R and L E Samuels 1971, *Foundry metallography* [annotated metallographic specimens: special series—studies in technology] (Betchworth) [as referenced in Unglik 1990].

Bronson B 1999, 'The transition to iron in ancient China', in V C Pigott (ed), *The archaeometallurgy of the Asian Old World* (Philadelphia: MASCA Research Papers in Science and Archaeology 16), 177–193.

Burger W 1976, *Ching cash until 1735* (Taipei).

Chen Hao 2002, 'Jiangbei tieqian jian ruogan wenti tansuo' [On the iron coin mints of the Jiangbei region], *Zhongguo Qianbi* [*China Numismatics*] 2002/1, 11–16.

Craddock P T, Wayman M L and Jull T In press, 'The radiocarbon dating and authentication of iron artefacts', *Radiocarbon*

Evrard R and Descy A 1948, *Histoire de l'Usine des Vennes* (Liège) [as referenced in Rostoker and Bronson 1990].

Golas P J 1999, 'Mining', in J Needham (ed), *Science and Civilization in China* 5(XIII) (Cambridge).

Han Rubin 1996, 'The development of Chinese ancient iron blast furnace', *Forum for the 4th International Conference on the Beginning of the Use of Metals and Alloys (BUMA-IV)* (Shimane, Japan), 151–174.

Hansen M and Anderko K, 1958 *Constitution of Binary Alloys* (New York).

Hartwell R 1962, 'A revolution in the Chinese iron and coal industries during the Northern Sung, 960–1126 AD', *Journal of Asian Studies* 21, 153-162.

Hartwell R 1963, Iron and early industrialism in eleventh-century China. Unpublished PhD thesis, University of Chicago [as referenced by Wagner (2001)].

Hartwell R 1966, 'Markets, technology and the structure of enterprise in the development of 11th century Chinese iron and steel industry', *Journal of Economic History* 26(1), 29–58.

Hartwell R 1967a, 'The evolution of the early Northern Sung monetary system, AD 960–1025', *Journal of the American Oriental Society* 87, 280–289.

Hartwell R 1967b, 'A cycle of economic change in imperial China: Coal and iron in northeast China 750-1350', *Journal of the Economic and Social History of the Orient* 10, 102–159.

Henger G W 1970, 'The metallography and chemical analysis of iron-base samples dating from antiquity to modern times', *Historical Metallurgy* 4(2), 45–52; erratum 1971, 5(1), 11.

Hua Jue-ming, 1983, 'The mass production of iron castings in ancient China', *Scientific American* 248, 107–114.

Jin Xiaochun, Jiang Yonghu, Cheng Jianzhong and Yang Jianxin

2000, 'Anhui Huaining Shankou zhencun zhuqian yizhi ji Tong'an jian zhi kaocha' [An investigation of the Tong'an mint site at Shankou zhencun, Huaining, Anhui province] , *Zhongguo Qianbi* [*China Numismatics*] 2000/3, 44–45.

Li Jinghua 1996, 'The excavation and study of iron smelting sites in Henan of Han dynasty, China', *Bulletin of the Metals Museum* 25, 14–35.

Liu Sen, 1997, *Zhongguo tie qian* [*Iron coinage in China*] (Beijing).

Peng Xinwei 1965, *Zhongguo Huobi Shi*. Published in 1984 as E H Kaplan (trans), *A monetary history of China*, vol 1 (Western Washington University: East Asian Research Aids and Translations 5).

Pfannenschmidt C W 1977, *Die Anwendung des Holzkohlenhochofens Seit ende des 16 Jahrhunderts zur Erzeugung von Gusswaren Erster Schmeltzung und die Spatere Zweite Schmelzung in Flamm-und Kupolofen Bis Mitte des 19 Jahrhunderts* (Dusseldorf: Verein Deutscher Eisenhuttenleute Fachausschussbericht 9.007) [as referenced in Rostoker and Bronson 1990].

Pinel M L, Read T T and Wright T A 1938, 'Composition and microstructure of ancient iron castings', *Transactions of the American Institute of Mining and Metallurgical Engineers* 131, 174–94.

Qui Shihua and Cai Lianzhen 1986, 'Woguo gudai yetie ranliao de tan-shisi jianding' [use of radiocarbon dating to determine the fuel used in ancient Chinese iron-smelting], in Wang Zhongshu and An Zhimin (eds), *Zhongguo kaoguxue yanjiu* (Beijing), 359–63.

Read T T 1939–40, 'The earliest industrial use of coal', *Transactionsof the Newcomen Society* 20, 119–33.

Rehder J E 1987, 'The change from charcoal to coke in iron smelting', *Historical Metallurgy* 21, 37–43.

Rostoker W 1986, 'Troubles with cast iron cannon', *Archeomaterials* 1, 69–90.

Rostoker W Bronson B, Dvorak J and Shen G 1983, 'Casting farm implements, comparable tools and hardware in ancient China', *World Archaeology* 15(2), 196–210.

Rostoker W, Bronson B and Dvorak J 1984, 'The cast iron bells of China', *Technology and Culture* 25, 750–67.

Rostoker W and Bronson B 1990, *Pre-industrial iron* (Philadelphia: Archeomaterials monograph 1).

Till B and Swart P 1993, 'Cast iron statuary of China', *Orientations* (August 1993), 40–45.

Tylecote R F 1976, *A History of Metallurgy* (London).

Tylecote R F 1991, 'Iron in the Industrial Revolution', in J Day and R F Tylecote (eds), *The Industrial Revolution in Metals* (London).

Unglik H 1990, *Cast irons from Les Forges du Saint-Maurice, Quebec: A metallurgical study* (Ottawa: Studies in Archaeology, Architecture and History, National Historic Parks and Sites).

Von Glahn R 1996, *Fountain of fortune: money and monetary policy in China, 1000–1700* (Berkeley).

Wagner D B 1989, *Toward the reconstruction of ancient Chinese techniques for the production of malleable cast iron* (Copenhagen: East Asian Institute Occasional Paper 4).

Wagner D B 1993, *Iron and steel in ancient China* (Leiden).

Wagner D B 1999, 'The earliest use of iron in China', in S M M Young, A M Pollard, P Budd and R A Ixer (eds), *Metals in Antiquity* (Oxford: BAR International Series 792), 1–9.

Wagner D B 2000, 'Chinese monumental iron castings', *Journal of East Asian Archaeology* 2(3/4), 199–224.

Wagner D B 2001, 'Blast furnaces in Song/Yuan China', *East Asian Science, Technology and Medicine*, 18, 41–74. See also pp 25–37 below.

Wang Shengduo 1998, 'Shaanxi zhuqianjian kao' [The mints of Shaanxi], *Zhongguo Qianbi* [*China Numismatics*] 1998/1, 1–8.

Wayman M L Lang J and Michaelson C forthcoming, The metallurgy of cast iron statuary.

Williams, J (ed) 1997, *Money a history* (London).

Yan Fushan (ed) 2001, *Liang Song tie qian* [*Iron coinage of the Northern and Southern Song*] (Xi'an).

Yang Lien-sheng 1952, *Money and credit in China: A short history* (Cambridge, Mass): Harvard-Yenching Institute Monograph series 12).

Zhou Weirong 1999, 'Shilun woguo gudai tieqian de qiyuan [On the origins of iron coinage in ancient China]', *Zhongguo Qianbi* [*China Numismatics*] 1999/1, 22–26.

The authors

Michael L Wayman is a Professor of Metallurgy at the University of Alberta in Edmonton, Canada. His research interests lie in archaeometallurgy and materials characterization with recent emphasis on early ferrous materials.

Address: Department of Chemical and Materials Engineering, University of Alberta, Edmonton, Alberta, Canada T6G 2G6.

e-mail: mwayman@ualberta.ca

Helen Wang is Curator of East Asian Money in the Department of Coins and Medals, British Museum. Her recent work has focused on Sir Aurel Stein and the coins he collected in Xinjiang, China.

Address: Department of Coins and Medals, British Museum, London WC1B 3DG, UK.

e-mail: hwang@thebritishmuseum.ac.uk